Characterization and Application of Dichroic Filters in the 0.1–3-THz Region

Carsten Winnewisser, Frank T. Lewen, Michael Schall, Markus Walther, and Hanspeter Helm

***Abstract*—Low-loss dichroic filters, a subgroup of frequency-selective components, have been characterized by terahertz time-domain spectroscopy in the region from 0.1 to 3 THz and with Fourier transform spectroscopy. The two data sets are fully consistent. The time-domain spectrometer is used to investigate the phase velocity behavior of dichroic filters. The dichroic filters have various applications in frequency mixing, multiplying, and diplexing experiments. In a novel application, cascaded filters were used to limit the terahertz pulse bandwidth and to monitor molecular transitions of atmospheric water vapor in a selected frequency band.**

***Index Terms*—Frequency selective surfaces and components, submillimeter waveguide arrays, dichroic filters, evanescent modes, terahertz time-domain spectroscopy, time domain measurements, spectral analysis.**

I. Introduction

DICHROIC filters are a subgroup of frequency-selective components (FSC's) [1], which have found widespread application from the microwave to the near-infrared spectral region. They are used as filters [2], [3], in frequency multipliers [4]–[6], as laser-cavity output couplers [7], or Fabry–Perot interferometers [8]. FSC's consist of periodically perforated components, where the shape and arrangement of the apertures determine the filter characteristics. This paper covers three main experimental topics. In Section III-A, we extend our previous work [9], [10] on dichroic filters and compare our terahertz–time-domain spectroscopy (THz–TDS) measurement of a dichroic filter with a cutoff frequency at 1.11 THz with Fourier transform spectroscopy (FTS). FTS extends the measured transmittance behavior of this dichroic filter to 200 THz. From the FTS measurements, the value for the filter's porosity is determined. In Section III-B, the frequency-dependent phase and group velocities in dichroic filters as determined from the experimental THz–TDS data are discussed. THz–TDS allows us to determine the phase shift directly because the electrical field strength of the terahertz pulse $E(t)$ is recorded. In this respect THz–TDS assumes the function of a network analyzer in the terahertz region.

Manuscript received March 17, 1999. This work was supported by the Deutsche Forschungsgemeinschaft under Contract SFB 276 and Contract SFB 301.

C. Winnewisser is with the Freiburg Materials Research Center, University of Freiburg, D-79104 Freiburg, Germany.

F. T. Lewen is with the I. Physikalisches Institutat University of Cologne, D-50923 Cologne, Germany.

M. Schall and M. Walther are with the Department of Molecular and Optical Physics, University of Freiburg, D-79104 Freiburg, Germany.

H. Helm is with the the Department of Molecular and Optical Physics, Albert-Ludwigs University, D-79104 Freiburg, Germany.

Publisher Item Identifier S 0018-9480(00)02424-8.

A novel application of commercially available freestanding electroformed nickel sheets from Stork Screens Company, Boxmeer, The Netherlands, as a dichroic filter is discussed in Section III-C. Cascaded filters allow time-resolved measurements in a narrow frequency bandwidth. As an example, we present rotational transitions of the H_2O molecule in the frequency bandwidth between 1.6–1.8 THz. Broad-band measurements have previously been performed by van Exter *et al.*in the region between 0.5–1.4 THz with a terahertz time-domain spectrometer [11].

II. Dichroic Filters

The most common dichroic filter consists of a metal plate composed of an equilateral array of hexagonally close-packed circular waveguides. The general parameters of these filters are briefly discussed here. A more detailed description of the transmittance behavior of FSC's is given by the mode-matching theory of Chen [14]. The cutoff frequency for an infinitely long cylindrical waveguide is defined by the hole diameter d

$$\nu_c^{\inf} = 1.841\frac{c}{\pi d} \tag{1}$$

where c is speed of light in free space [12]. The hexagonal hole array of the dichroic filter represents a two-dimensional grating, which will force electromagnetic (EM) waves with frequencies above

$$\nu_{\text{diff}} = \frac{2c}{s\sqrt{3}} \tag{2}$$

to be diffracted into the first diffraction lobe [13], where s is the hole spacing. For frequencies much higher than the diffraction limit, the filter transmission rises to the porosity value, which is the geometric ratio of opening to blockage area, given by

$$T_{\text{porosity}} = \frac{\pi}{2\sqrt{3}}\left(\frac{d}{s}\right)^2. \tag{3}$$

The length l of the waveguide determines how strongly waves in an evanescent mode are attenuated, thus controlling the sharpness of the waveguide cutoff characteristic.

III. Experiment

The filter transmission characteristics were measured by an electrooptic (EO)-sampling procedure and a conventional terahertz–time-domain spectrometer described in [15] and [16], re-

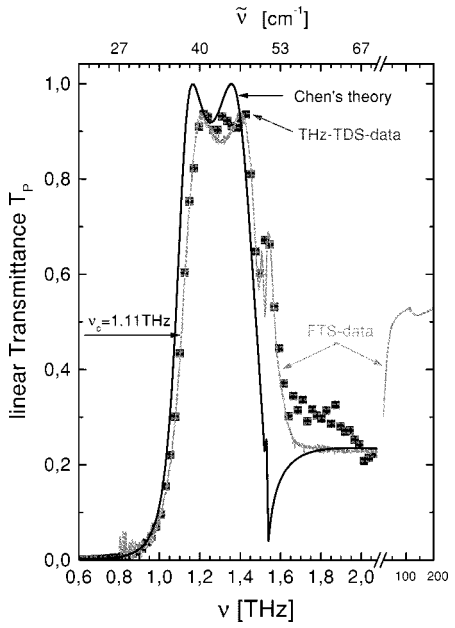

Fig. 1. Power transmittance T_P of the terahertz dichroic filter #1 measured with a terzhertz–time-domain spectrometer (squares) is shown together with the theoretical transmittance data (black line) obtained by Chen's transmission theory [14], [15]. The transmittance of the dichroic filter measured with a Fourier transform spectrometer is shown as a gray line.

spectively.[1] The electrical field strength of the terahertz pulse $E(t)$ is recorded with and without the FSC placed in the path of the terahertz beam. By taking the Fourier transform of time-domain data $E(t)$, one obtains the complex amplitude spectrum $E(\nu)$ in the form of both magnitude $|E(\nu)|$ and phase $\phi(\nu)$.

The power transmittance $T_P(\nu)$ of the filters is calculated by taking the square of the ratio between the Fourier transformed sample and reference data. The phase shift is defined as $\Delta\phi(\nu) = \phi_{\rm sample}(\nu) - \phi_{\rm ref}(\nu)$ [15].

A. Power Transmittance

Fig. 1 compares the experimental power transmittance (squares) obtained for filter #1 [10] with the theoretical transmittance (black line) calculated from the theory given by Chen [14], [15]. There is a slight shift toward a higher cutoff frequency compared to the theoretical data. This is likely due to the slightly conical shape of the drilled holes and to ohmic losses effects, which are not included in Chen's theory.

To independently confirm our EO-sampling THz–TDS results, we performed a measurement of this filter using a commercial Fourier transform spectrometer. This transmittance curve is presented as the gray line in Fig. 1 and shows very good agreement with our THz–TDS measurements.

Below the cutoff frequency, the dichroic filter acts like a mirror. Due to the finite filter length l, an evanescent transmittance value of $T_P < 10^{-3}$ is observed below 0.6 THz [10].

At higher frequencies, where diffraction losses occur, the transmittance drops below the porosity value down to about $T_P \approx 0.2$ and stays almost constant up to 10 THz. From here on, the transmittance slowly approaches the porosity value of

[1]In [15], the phase shift $\Delta\phi\nu$ should read $\Delta\phi\nu = \phi_{\rm sample}(\nu) - \phi_{\rm ref}(\nu)$ and line three of Table I should read: filter C, $l = 0.290$ mm, $d = 0.235$ mm, $s = 0.297$ mm

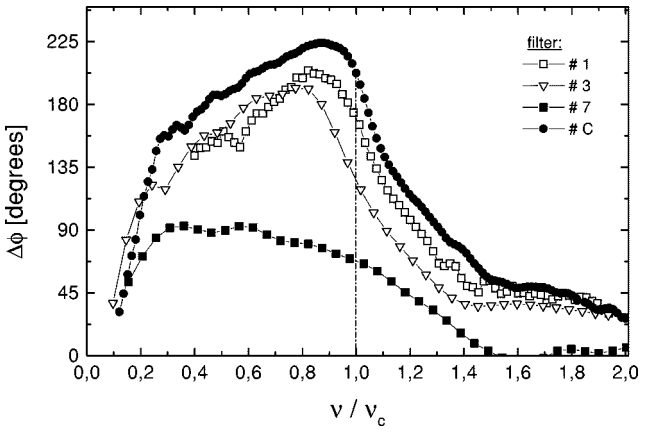

Fig. 2. Phase behavior of four dichroic filters, which are listed in Table I.

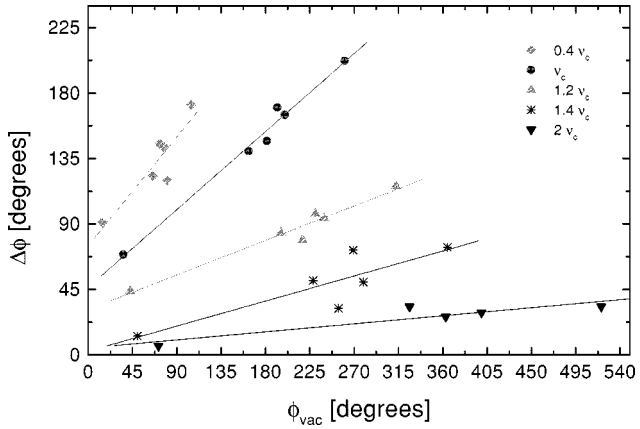

Fig. 3. Measured phase shifts $\Delta\phi$ at selected frequencies $q \cdot \nu_c$ for six different dichroic filters are shown versus the vacuum phase shift $\phi_{\rm vac}$ when propagating the thickness of each individual filter.

≈0.52 above 100 THz. The theoretical porosity value for filter #1 according to (3) is $T_{\rm porosity} = 0.5$.

B. Phase Shift

In this section, we discuss the phase-shift characteristics of six dichroic filters, the transmission characteristics of which we presented in [10] and [15]. The mechanical parameters of four of these filters are specified in Table I and their phase characteristics are plotted versus frequency in Fig. 2. The frequency scale is normalized to the experimental cutoff frequency ν/ν_c.

Positive phase differences $\Delta\phi(\nu)$ imply that the frequency component of the probe pulse transits the filter faster than does the appropriate component of the reference pulse. At high frequencies $\nu/\nu_c \gg 1$, the phase shift difference $\Delta\phi(\nu)$ drops to zero, indicating that the phase velocity $v_{\rm ph}(\nu)$ approaches the speed of light c. This is a feature that is well known from waveguide theory [12]. In order to examine the phase shift behavior, we plot $\Delta\phi$ at selected frequencies $q\nu_c$, where q is a dimensionless parameter. Fig. 3 shows these phase shifts $\Delta\phi(q\nu_c)$ for q between 0.4– 2.0 versus the phase shift in free space

$$\phi_{\rm vac} = qk_c l = \frac{2\pi q \nu_c l}{c} \tag{4}$$

where $\phi_{\rm vac}$ is the phase shift encountered when propagating the distance l in free space and k_c is the wavenumber at cutoff.

TABLE I
PARAMETERS OF THE DICHROIC FILTERS. ν_c IS THE EXPERIMENTAL CUTOFF FREQUENCY AT -3 dB RELATIVE TO PEAK TRANSMITTANCE. THE FILTER TAGGING CORRESPONDS TO THE LABELS USED IN [10] AND [15]

#	ν_c [GHz]	ν_{center} [GHz]	3 dB bandwidth [%]	max. T_P [dB]	l [μm]	d [μm]	s [μm]
dichroic filters							
1	1112	1300	30	-0.3	153	168	226
3	242	300	36	> -0.2	700	740	970
7	228	290	44	> -0.2	125	740	970
C	773	945	36	> -0.2	290	235	297
electroformed nickel mesh							
8	1600	1700	12	-1	120	88	179

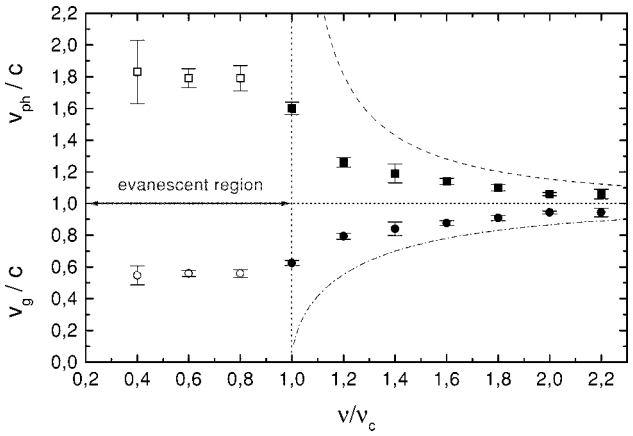

Fig. 4. Phase and group velocity of dichroic filters normalized to the speed light in free space c plotted versus the frequency normalized to the cutoff frequency. The dashed and dashed–dotted curves show the theoretical phase and group velocities of an infinitely long lossless waveguide, respectively.

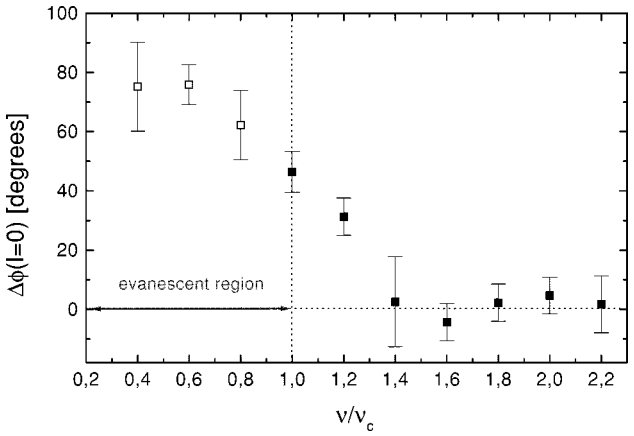

Fig. 5. Phase-shift characteristic of an infinitely thin dichroic filter plotted versus the normalized frequency.

The data plotted in this manner indicate a linear relation between the phase shift $\Delta\phi$ encountered in the filter and the phase ϕ_{vac}. If the filter introduces no additional phase shift, the slope m in Fig. 3 would be zero, i.e., the phase velocity v_{ph} would be equal to the speed of light c. A slope $m > 0$ corresponds to a phase velocity $v_{\text{ph}} = (m+1)c > c$. The data points of each frequency set $q \cdot \nu_c$ were fitted to a straight line and the slope m and the intercept of the y-axis were determined.

In Fig. 4, we show the derived phase velocities (squares) versus the normalized frequency. At high frequencies, the phase velocity approaches the speed of light in free space c, while the phase velocity rises to values around $1.6c$ at the cutoff. The phase velocity in an infinitely long and lossless waveguide is known to follow the equation $v_{\text{ph}} = c/\sqrt{1-(\nu_c/\nu)^2}$ [12]. This result is plotted as a dashed line in Fig. 4. The group velocity $v_g = c^2/v_{\text{ph}}$ is also shown in Fig. 4.

In Fig. 5, the intercept for $\phi_{\text{vac}} = 0$ of the linear fits to the data in Fig. 3 are shown as a function of ν/ν_c. The intercept values correspond to the phase shifts $\Delta\phi$ an EM wave would encounter for an infinitely thin $(l \to 0)$ dichroic filter. Such a filter electrically approximates the behavior of a purely inductive grid (high-pass filter) [2], called a frequency-selective surface (FSS) [1]. In the case of a purely inductive grid, the phase shift changes from 90° below the cutoff, to 45° at the cutoff frequency, and approaches zero at high frequencies.

In the following, we discuss the evanescent mode propagation through the dichroic filters. Within the evanescent region, we have a superposition of exponentially decaying waves. When transmitting an EM pulse in the evanescent region, the higher frequency components of the pulse will be attenuated less than the lower ones. This problem has been discussed in several recent studies of the analogy between quantum tunneling of a particle and the time delay experienced by an evanescent EM wave packet [17]–[19]. Conventional studies of the time-delay effect monitor an amplitude modulated wave passing through a restricted waveguide [20]. These data are complicated due to reflections arising at the geometrical boundaries, and they do not yield easily interpretable results [18].

Fig. 3 attempts to separately analyze the boundary effects posed by the different filters from effects of the evanescent mode behavior in the waveguide array. As evident from Fig. 3, the different filters share a common linear dependence of $\Delta\phi$ versus ϕ_{vac}. We interpret the slope of these lines as the dependence of the phase velocity on the normalized frequency. Below the cutoff frequency, we observe the phase velocity to be constant, at around $1.8c$, albeit with the error bars reaching as high as $\pm 11\%$ (see Fig. 4). We also interpret the intercept for $\phi_{\text{vac}} = 0$ (equivalent to $l \to 0$) as the change in phase resulting from the

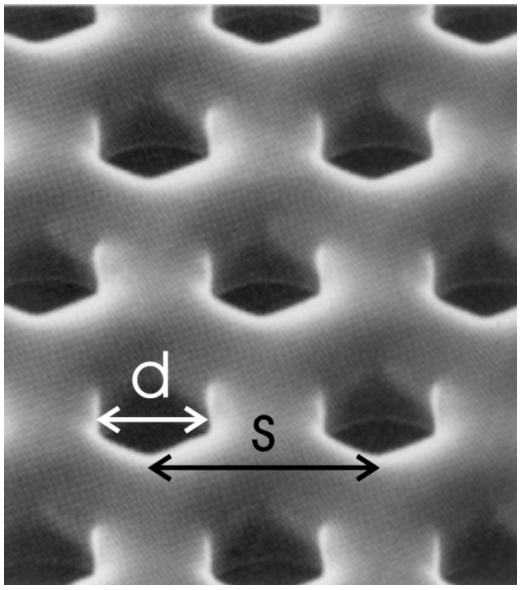

Fig. 6. Microscope image of an electroformed nickel screen with hole diameters $d = 88\ \mu$m, and a hole spacing $s = 179\ \mu$m. The screen thickness is 120 μm.

boundary problem alone—which still exists for an infinitely thin filter (see Fig. 5).

While we have not carried out these measurements with the time-delay problem in mind, we now feel that the use of narrow-bandwidth terahertz pulses in THz–TDS is a possible route for further experiments in this domain.

C. Stork Screens as Dichroic Filters

The use of Stork Screen mesh as frequency filter in the far infrared (FIR) has been suggested by Huggard *et al.* [21]. In Fig. 6, a segment of a mesh Nova 135ED with hexagonal apertures is shown. We have measured the filter transmission characteristics of such filters using our terahertz–time-domain spectrometer operating between 0.1–3 THz [16].

The power transmittance $T_P(\nu)$ obtained from this filter is shown in Fig. 7. The cutoff frequency is at $\nu_c = 1.6$ THz. The peak of the transmittance of about 80% occurs at 1.7 THz. The passband ends around 1.85 THz, which is consistent with the diffraction limit of $\nu_{\text{diff}} = 1.9$ THz, as given by (2).

By inserting this mesh in the terahertz-beam path, one can narrow a broad-band terahertz pulse. Cascading two identical "Stork" filters separated by 2 cm creates a bandpass from 1.6 to 1.8 THz with a peak transmittance of about $T_P^2 \approx 0.64$, which can be used for spectroscopic purposes. In this manner, it is possible to measure the response of an ensemble of molecules to the electric dipole interaction of a narrow-bandwidth pulsed EM field.

In Fig. 8, the sample trace of two cascaded "Stork" filters in the presence of laboratory-air water vapor is shown. The inset reveals electrical dipole oscillations due to rotational transitions that lie in the passband of the filters. Fourier transforming the time-domain data shown in the inset of Fig. 8 reveals the water vapor transitions $2_{1,2}-1_{0,1}$ at 1.67 THz, $6_{2,4}-6_{1,5}$ at 1.79 THz, and $7_{3,4} - 7_{2,5}$ at 1.8 THz in the frequency domain, shown in Fig. 9. The transition nomenclature is $J(K_a, K_c)$ [22].

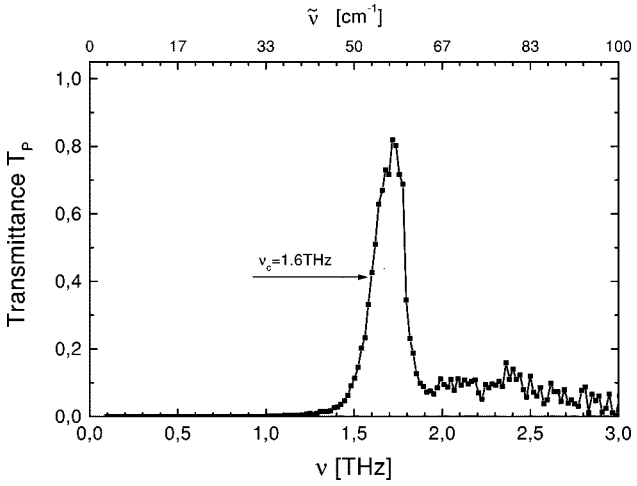

Fig. 7. Filter transmission of a single Stork screen with an experimental cutoff frequency of 1.6 THz at -3-dB peak transmittance.

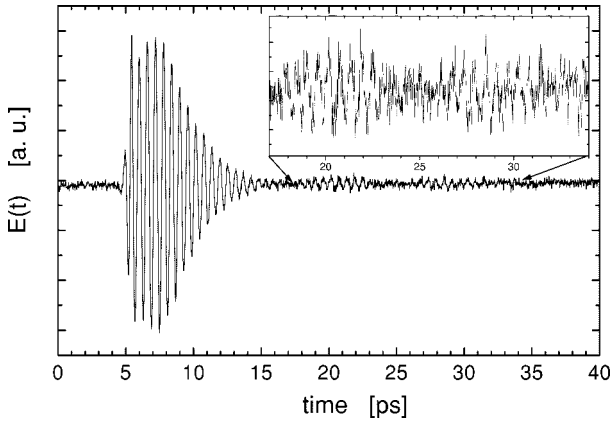

Fig. 8. Sample trace of the two cascaded Stork screens. The inset shows the time interval between 17–34 ps with an expanded amplitude scale. The oscillations of the electrical-field amplitude are due to water vapor rotational transitions that lie within the bandpass of the cascaded filters.

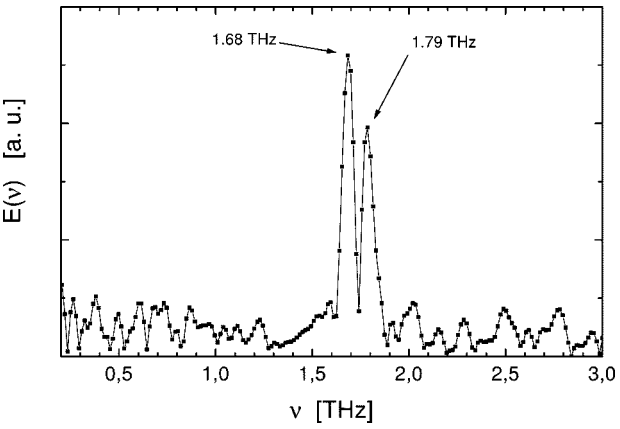

Fig. 9. Fourier transformed data of the inset of Fig. 8. The three water transitions are observed as two absorption lines. The peak at 1.79 THz consists of two blended water lines at 1.79 and 1.8 THz.

It should be mentioned that an alternative and elegant way to produce tunable narrow bandwidth terahertz pulses has been recently presented by Weling *et al.*[23]. This technique involves the optical heterodyning of two linearly chirped broad-band

pulses at $\lambda = 800$ nm to produce a quasi-sinusoidal intensity modulation in the terahertz region.

IV. Conclusion

In this paper, we have compared THz–TDS and FTS measurements of the transmittance function of dichroic filters, and find that the two data sets agree very closely. We show that TDS gives direct access to the phase velocity in the bandpass and in the evanescent region of the filter, acting as a network analyzer in the terahertz regime. Finally, we used cascaded filters for narrow bandwidth measurements with pulsed terahertz radiation.

Acknowledgment

The authors would like to thank M. Lock, The University of Giessen, Giessen, Germany, and B. Schubach, University of Freiburg, Freiburg, Germany, who carried out the measurements in the FIR and mid infrared (MIR) of the dichroic filter #1 with Bruker 4IFS 120HR and Bruker IFS 66v/S FT spectrometers, respectively. The authors also thank Stork Screens B.V., Boxmeer, The Netherlands, for providing samples of the precision printing screens.

References

[1] P. F. Goldsmith, *Quasioptical Systems*. Piscataway, NJ: IEEE Press, 1997.
[2] R. Ulrich, "Interference filters for the far infrared," *Appl. Opt.*, vol. 7, pp. 1987–1995, 1968.
[3] V. P. Tomaselli, D. C. Edewaard, P. Gillan, and K. D. Möller, "Far-infrared bandpass filters form cross-shaped grids," *Appl. Opt.*, vol. 20, pp. 1361–1366, 1981.
[4] J. W. Archer, "A novel quasi-optical frequency multiplier design for millimeter and submillimeter wavelengths," *IEEE Trans. Microwave Theory Tech.*, vol. MTT-32, pp. 421–426, 1984.
[5] J. W. Archer, "Correction to 'a novel quasioptical frequency multiplier design for millimeter and submillimeter wavelengths'," *IEEE Trans. Microwave Theory Tech.*, vol. MTT-33, pp. 741–741, 1985.
[6] F. Lewen, S. P. Belov, F. Maiwald, T. Klaus, and G. Winnewisser, "A quasioptical multiplier for terahertz spectroscopy," *Z. Nat.Forsch. A, Phys. Phys. Chem. Kosmophys.*, vol. 50A, pp. 1182–1186, 1995.
[7] D. A. Weitz, W. J. Skocpol, and M. Tinkham, "Capacitive-mesh output couplers for optically pumped far-infrared lasers," *Opt. Lett.*, vol. 3, pp. 13–15, 1978.
[8] R. D. Rawcliffe and C. M. Randall, "Metal mesh interference filters for the far infrared," *Appl. Opt.*, vol. 6, pp. 1353–1358, 1967.
[9] C. Winnewisser, F. Lewen, J. Weinzierl, and H. Helm, "Frequency-selective surfaces analyzed by THz time-domain spectroscopy," in *Proc. IEEE 6th Int. Terahertz Electron. Conf.*, 1998, pp. 196–198.
[10] ——, "Transmission features of frequency-selective components in the far infrared determined by terahertz time-domain spectroscopy," *Appl. Opt.*, vol. 38, pp. 3961–3976, 1999.
[11] M. van Exter, C. Fattinger, and D. Grischkowsky, "Terahertz time-domain spectroscopy of water vapor," *Opt. Lett.*, vol. 14, pp. 1128–1130, 1989.
[12] N. Marcuvitz, *Waveguide Handbook*. New York: McGraw-Hill, 1951.
[13] L. A. Robinson, "Electrical properties of metal-loaded radomes," Wright-Patterson Air Force Base, OR, Tech. Rep. WADD-TR-60-84 (NTIS AD-249 410), 1960.
[14] C.-C. Chen, "Transmission of microwave through perforated flat plates of finite thickness," *IEEE Trans. Microwave Theory Tech.*, vol. MTT-21, pp. 1–7, Jan. 1973.
[15] C. Winnewisser, F. Lewen, and H. Helm, "Transmission characteristics of dichroic filters measured by THz time-domain spectroscopy," *Appl. Phys. A, Solids Surf.*, vol. 66, pp. 593–598, 1998.
[16] M. Schall, H. Helm, and S. Keiding, "Far infrared properties of electro-optic crystals measured by THz time-domain spectrocopy," *Int. J. Infrared Millim. Waves*, vol. 20, pp. 595–608, 1999.
[17] T. Hartman, "Tunneling of a wave packet," *J. Appl. Phys.*, vol. 33, pp. 3427–3433, 1962.
[18] T. Martin and R. Landauer, "Time delay of evanescent electromagnetic waves and the analogy of particle tunneling," *Phys. Rev. A, Gen. Phys.*, vol. 45, pp. 2611–2617, 1992.
[19] A. Enders and G. Nimtz, "Evanescent-mode propagation and quantum tunneling," *Phys. Rev. E*, vol. 48, pp. 632–634, 1993.
[20] A. Ranfagni, D. Mugnai, P. Fabeni, and G. P. Pazzi, "Delay-time measurements in narrowed waveguides as a test of tunneling," *Appl. Phys. Lett.*, vol. 58, pp. 774–776, 1991.
[21] P. G. Huggard, M. Meyringer, D. Schilz, K. Goller, and W. Prettl, "Far-infrared bandpass filters from perforated metal screens," *Appl. Opt.*, vol. 33, pp. 39–41, 1994.
[22] J. K. Messer, F. C. DeLucia, and P. Helminger, *Int. J. Infrared Millim. Waves*, vol. 4, pp. 505–539, 1983.
[23] A. S. Weling and D. H. Auston, "Novel sources and detectors for coherent tunable narrow-band terahertz radiation in free space," *J. Opt. Soc. Amer. B, Opt. Phys.*, vol. 13, pp. 2783–2791, 1996.

Carsten Winnewisser was born in Durham, N.C. He received the diploma and Ph.D. degrees in physics from the University of Freiburg, Freiburg, Germany, in 1994 and 1999, respectively, and the medical physics and techniques degree from the University of Kaiserslautern, Kaiserslautern, Germany, in 1997.

From 1995 to 1999, he was involved with the generation, detection, and application of terahertz pulses in the Department of Molecular and Optical Physics, University of Freiburg. He is currently a Post-Doctoral Fellow at the Freiburg Materials Research Center, University of Freiburg. His current interests lie in the application of photonic structures in the far infrared and optical region.

Dr. Winnewisser is a Fellow of the German Physical Society (DPG).

Frank T. Lewen received the diploma and Ph.D. degrees in physics from the University of Cologne, Cologne, Germany, in 1990 and 1993, respectively.

From 1990 to 1994, he was with the Kölner Observatorium für Submillimeter und Millimeter Astronomie (KOSMA) Receiver Group, where he constructed a 660-GHz heterodyne receiver system for the Gornergrat Observatory (near Zermatt, Swiss Alps). Since 1994, his research interests includes terahertz sources and high-resolution spectrometers for molecular spectroscopy. He successfully developed phase-locked-loop electronics and terahertz–harmonic mixers for phase stabilizing of backward-wave oscillators (BWO's) up to 1.3 THz and precise frequency control circuits for far infrared laser systems. He is currently designing broad-band tunable frequency multipliers in the frequency range from 1 to 1.6 THz with planar Schottky barrier diodes. He is the Head of the Cologne Terahertz Spectroscopy Group, which operates ultrahigh-resolution spectrometers in the 0.1–2-THz region.

Dr. Lewen is a member of the German Physical Society (DPG).

Michael Schall received the diploma degree in molecular and optical physics from the University of Freiburg, Freiburg, Germany, in 1996, and is currently working toward the Ph.D. degree at the University of Freiburg.

His current interest includes transient terahertz time-domain spectroscopy of semiconductors.

Markus Walther received the bachelor degree in physics from the University of Freiburg, Freiburg, Germany, in 1994, and is currently working toward the Ph.D. degree in terahertz time-domain-spectroscopy of biomolecules and semiconductors at the University of Freiburg.

Hanspeter Helm was born in Austria. He received the Ph.D. degree from the University of Innsbruck, Innsbruck, Austria, in 1973.

Following a Post-Doctoral Fellowship at the Australian National University, Canberra, Australia, he joined SRI International in 1978. Since 1994, he has been the Head of the Department of Molecular and Optical Physics, Albert-Ludwigs University, Freiburg, Germany.

Dr. Helm is a Fellow of the American Physical Society.